Nature-inspired Apatite Production: Steam Processing of Calcium Carbonate and Tricalcium Phosphate Nanosized Powder Blends

Aiga Anna JOKSA *, **Karlis Agris GROSS**

Institute of Materials and Surface Engineering, Faculty of Materials Science and Applied Chemistry, Riga Technical University, Riga, LV-1048, Latvia

Green production of materials is crucial to protect the environment. In this article, a low-temperature steam synthesis strategy for apatite production is shown for limiting chemical pollution and enabling the control of crystallinity. Steam processing produced apatite from calcium carbonate and tricalcium phosphate nanosized powders. Interdiffusion between amorphous precursors gave hydroxyapatite accompanied by calcium-deficient hydroxyapatite. This study unfolds the potential of hydrothermal processing in steam as a synthesis strategy that has been forgotten since the 1950s showing where two solid nanosized powders react to form a new product without creating waste, thereby emulating the clean processing route found in nature. This research reopens the consideration of steam processing for more chemically diverse alternatives and processing of various calcium resources readily available in nature, such as eggshell waste, for greener production. Furthermore, it presents a rarely found combination of apatite forms.

Keywords: amorphous, calcium carbonate, tricalcium phosphate, crystallization, hydrothermal.

1. INTRODUCTION

Apatite compounds are formed and deposited in biological organisms, such as mitochondria cells, bone, and teeth [1]. The similarity of apatite to the inorganic part of the bone contributes to the synthesis of apatite compounds for biomedical purposes. Here, we mimic biomineralization in nature using hydrothermal conditions for the crystallization of calcium carbonate and tricalcium phosphate nanosized blends to produce high-crystallinity hydroxyapatite. This is the first study to use amorphous nanosized starting powders a mix of calcium carbonate and tricalcium phosphate powders to produce apatite via steam processing.

Synthesis is usually environmentally unfriendly due to accompanying chemicals in the reagents that end up as by-products. Efforts to develop environmentally clean industrial processes and the use of green chemistry principles for sustainability are guiding greener production processes. Various events in nature form hard minerals in hydrothermal conditions. Sediments transform into sedimentary rocks under pressure and temperature: sediments are compacted, fluids fill the interstices between loose particles, and form a hardened rock [2]. As a result, pollutant chemicals are avoided, and water is an eco-friendly chemical. We found it interesting to see if this transformation phenomenon could be used as a new synthesis strategy for apatite production from calcium carbonate and tricalcium phosphate compacted nanosized powders.

The sedimentary rock formation has inspired scientists to seek the benefits of hydrothermal conditions for synthesis and sintering. Hydrothermal synthesis, specifically of apatites, started in 1949 by Wyart who described the role of supercritical water [3] to show three reactions between a solid and steam to synthesize apatite [4]. In 1974 Skinner et al synthesized apatite in a faster reaction between more reactive phosphoric acid and calcium oxide [4] – several other studies were mentioned consisting of at least one solid phase and one solution. Zinc apatites from zinc-modified amorphous calcium phosphate powder showed concomitant substitution of Zn in the apatite structure from hydrothermal crystallization of amorphous phases [5].

There have been attempts to hydrothermally synthesize hydroxyapatite from eggshell waste [6], calcium carbonate in ammonium dibasic phosphate solution, and various ion-doped (Mg^{2+}, Sr^{2+}, Zn^{2+}) nitrate solutions [7, 8], zinc-doped hydroxyapatite [9] and fluoride-substituted calcium phosphates [10]. Despite the initial use of steam in hydrothermal synthesis [3], the liquid phase was adopted after 1952, presumably for the easier inclusion of a wider range of elements. This study returns to the use of steam to explore the synthesis inside a hydrothermal vessel. The use of nanosized reagent powders in this steam process is new and will provide faster reaction kinetics compared to previous studies.

Despite the multitude of studies on hydrothermal synthesis, less attention has been given to the compaction, and crystallization during the hydrothermal transformation of sediments to hardened rocks. A broad range of hydrothermal processes have been made available for low-temperature sintering: hydrothermal sintering (HS) [11], hydrothermal reaction sintering (HRS) [12], hydrothermal hot pressing (HHP) [13], reaction hydrothermal liquid-phase densification (rHLPD) [14] and energy-assisted hydrothermal sintering [15, 16], however, hydrothermal sintering of apatites is limited in two situations. In 1990,

---

* Corresponding author. Tel.: +371 27107475.
E-mail: *anna.joksa@outlook.com* (A.A. Joksa)

researchers in Estonia studied the hydrothermal reaction of hydroxyfluorapatite mineral with phosphoric acid [17] apatite (80 % purity) was obtained above 1300 °C. Twenty years later, Yanagisawa et al synthesized calcium-deficient hydroxyapatite (CDHA) by hydrothermal hot-pressing at 200 °C and achieved 80 % densification [18]. In 2016, the cold-sintering process (CSP) based on the same hydrothermal principles [19, 20] was developed, but has not been used to densify mixed $CaCO_3$ and $Ca_3(PO_4)_2$ powders yet. In this process, higher-density materials can be obtained even for metastable materials.

Calcium compounds form many polymorphs [3, 4, 19, 22, 23], thereby providing an opportunity to use reactants in different structural forms. Tricalcium phosphate exists in four allotropes [23 – 26]: the more common forms include amorphous tricalcium phosphate (highest energy), crystalline α-phase (higher energy) and crystalline β-phase (lower energy). To determine whether the reaction occurs between amorphous and crystalline phases, the reaction was conducted using both analogs β-tricalcium phosphate and crystalline calcium carbonate.

The objective of this study was to determine if pressed $CaCO_3$ and $Ca_3(PO_4)_2$ nanosized powders could be steam processed to a crystalline apatite. To study the reaction between amorphous and crystalline states of reactants, the authors chose wet synthesized precursors. The investigation with both states of reactants provided the basis to utilize commercially available powders and $CaCO_3$ biowaste for future studies. Steam processing was selected as the cleaner, waste-free (solid phases) synthesis route.

2. MATERIALS AND METHODS

2.1. Synthesis of calcium carbonate and tricalcium phosphate

The preparation of nanosized powders that were mechanically blended and prepared, as is described below. Nanosized amorphous phases provided a high surface area and the spherical shape allowed good powder packing. Amorphous calcium carbonate and amorphous tricalcium phosphate powders were synthesized by the wet precipitation method at room temperature.

Amorphous calcium carbonate (ACC) was synthesized without additional stabilizers or additives to evaluate the ability to retain pure ACC. The synthesis was carried out with 0.5 M NaOH (analytical grade, Enola) solution, 0.012 M $CaCl_2 \cdot 2H_2O$ (99 %, Penta), and 0.062 M dimethyl carbonate (99 %, Sigma-Aldrich) solution. Solution A consisted of calcium chloride and dimethyl carbonate dissolved in 1.2 liters of deionized water. Solution B was sodium hydroxide solution. Both solutions were combined and stirred for 3.5 minutes. During this time, hydrolysis of dimethyl carbonate took place, which was catalyzed by NaOH. After mixing, the solution was vacuum filtrated and washed with acetone (analytically pure > 99.8 %, Enola) and ethanol. After filtration, it was stored in a freezer for 24 h (-18.0 °C) and freeze-dried (Martin Christ Alpha 2-4 LSCplus, Osterode am Harz, Germany) for 24 h (0.01 mbar and 20 °C). As ACC is a metastable substance, it was stored immediately in a desiccator to prevent unwanted crystallization.

Amorphous tricalcium phosphate (ATCP) was synthesized in a basic environment. Solution A (dissolved in 250 ml deionized water) consisted of 0.12 M $(NH_4)_2 HPO_4$ (pure, Enola) and solution B (dissolved in 250 ml deionized water and 20ml ammonia) of 0.28 M $Ca(NO_3)_2 \cdot 4H_2O$ (pure, Enola) in ammoniacal water. The calcium and phosphorus molar ratio was 2.5:1. Solution A was poured into solution B. The resulting suspension was stirred for 10 minutes using a mechanical stirrer, filtered on a Buchner funnel, and washed with 1 liter of ammonia-water solution containing 5 ml of ammonia (25 % NH_4OH, for analysis EMSURE® ISO, Reag. Ph Eur and deionized water), 125 ml of deionized water and finally freeze-dried (Martin Christ Alpha 2-4 LSCplus, Osterode am Harz, Germany) for 24 h at 0.01 mbar pressure to obtain a dry powder.

2.2. Preparation of cold sintered pellets

Pellets were cold sintered at room temperature from mixed amorphous calcium carbonate and amorphous tricalcium phosphate in a Zwick/Roell mechanical testing machine. 0.5 g of powder was uniaxially pressed in a cylindrical hardened-steel die (Across International, Berkeley Heights, New Jersey, USA) at a 0.2 μN pre-load to establish the reference position. Loading up to 500 MPa used the position-controlled mode (3 mm/s), but the dwell phase used the force-controlled mode, where the load was automatically adjusted to 500 MPa during compression of the pellet during the holding time (10 min).

2.3. Steam processing

Steam processing differs from hydrothermal processing in that the material does not dissolve but is subjected to a specific atmosphere: in this case, steam and pressure. Steam processing of apatite was investigated in a reaction between calcium carbonate and tricalcium phosphate in different structural forms: amorphous and crystalline.

MIX-1 represented the pellet of mechanically blended and compressed amorphous calcium carbonate and amorphous tricalcium phosphate, while MIX-2 used crystallized forms of the reactant phases. Crystalline forms were produced by powder placement in a furnace already heated to 500 °C for calcium carbonate and 700 °C for tricalcium phosphate. Total incorporation of carbonate would produce a carbonated apatite:

$$CaCO_3 + 3Ca_3(PO_4)_2 + H_2O \rightarrow Ca_{10}(PO_4)6CO_3 + H_2O \quad (1)$$
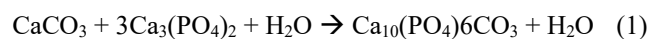
Initial powders were mixed in a 1:3 molar ratio, ground for 5 min, and then uniaxially densified in a hydraulic press for 10 min at 500 MPa to obtain a green body pellet, that was further placed in a hydrothermal vessel separated from 84.62 μl of deionized water. The hydrothermal vessel was placed in an oven and heated at 180 °C producing 1.0026 MPa pressure inside the vessel. The hydrothermal vessel was taken out of the oven after a 19 hour hold when the temperature was cooled down to at least 30 °C.

2.4. Characterization of initial powders and the final product

X-ray diffraction (XRD) data of amorphous calcium carbonate, amorphous tricalcium phosphate, and final

products were recorded by the D8 ADVANCE diffractometer (Bruker, USA) from 20° to 60° using Cu Kα radiation ($\lambda = 1.54$ Å generated at 40 mA and 40 kV) at a step size of 0.2°, to show the retention of the amorphous phase or formation of apatite from the steam processing. Rietveld's analysis determined the phase quantity (hydroxyapatite HA, calcium deficient hydroxyapatite CDHA, calcite, and β-tricalcium phosphate β-TCP) of hydrothermally processed amorphous and crystalline nanosized powders. Statistical errors were calculated using Round Robin data analysis and unit cell parameters were calculated by the least squares method using Profex software (Profex 5.0.1, Nicola Döbelin, Solothurn, Switzerland).

Fourier transform infrared spectroscopy (FTIR) was conducted with a Frontier FTI-IR/FIR Spectrometer (Perkin Elmer, USA) to show covalently active functional groups in sample powders, taken as a sign of phase purity. A total of 64 scans with absorption spectra were averaged from analysis in the transmission mode over a 400–4000 cm^{-1} range at a resolution of 4 cm^{-1}. A small amount (~ 2 mg) of powdered samples were ground in a mortar and combined with 250 mg of KBr by mixing into a homogeneous mixture and pressed into pellets. Obtained spectra were analyzed using SpectraGryph software (Dr. Friedrich Menges Software-Entwicklung, Oberstdorf, Germany). FTIR spectra deconvolution was conducted at 800–900 cm^{-1} range using curve-fitting by Lorentzian band shape to show carbonate incorporation into apatite structure: phosphate site (B-type) or OH- site (A-type).

The carbonate ion content was calculated from carbon mass fraction analysis. Data were recorded by the elemental analyzer EuroEA3000 (EuroVector, Pavia, Italy) coupled to a continuous flow isotope ratio mass spectrometer Nu-horizon (Nu Instruments, Wrexham, UK). To quantify the carbon, 1 mg of a powder predried at 105 °C for 2 h was weighed into a tin capsule. Each sample was analyzed in triplicate. For the quantification of the total amount of carbon five-point calibration graph method using L-glutamic acid (99.5 %, Sigma Aldrich, Japan) was used. For the accuracy control of the method, L-Glutamic acid

reference material (USGS-40 (Restek, Virginia, USA)) was used. Combustion and reduction reactors were used for the carbon analysis. $Mg(ClO_4)_2$ was used for water entrapment. The temperature regime was set at 1030 °C at the front and 650 °C at the back of the furnace.

From the obtained carbon mass fraction values, CO_3^{2-} quantity was calculated (Eq. 2):

carbonate ion quantity (mass % CO_3^{2-}) = carbon mass fraction (mass % C) · 60/12, (2)

where *carbon mass fraction* is the carbon content in samples determined by carbon mass fraction analysis, mass %.

Differential thermal analysis (DTA) was done to determine the crystallization temperature of amorphous calcium carbonate and amorphous tricalcium phosphate powders. The differential thermal analysis was performed by LABSYS EVO STA (SIMULTANEOUS THERMAL ANALYSIS) (Setaram Instruments, Caluire, France) device with a resolution of 0.4 µW/10 µW and accuracy is < 2 %. The samples were heated up from room temperature up to 800 °C with a heating rate of 10 °C min^{-1} using an argon flow of 60 ml min^{-1}. The samples were prepared by placing the powder in a sealed vacuum quartz ampoule and an empty quartz ampoule of equal mass was used as reference material. DTA analysis was used on 20–50 mg of powder.

The bulk density of pellets was calculated from the mass and the bulk volume. Sample mass was weighed on an analytical balance (KERN ABS220-4N) and bulk volume Vbulk was calculated from the measured height and diameter of a pellet (Eq. 3):

$$V_{bulk} = \pi d2h/4,$$ (3)

where d and h are pellet diameter and height, respectively.

3. RESULTS

3.1. Physicochemical characterization of synthesized powders and cold-pressed pellets

Fig. 1 a shows the XRD diffraction pattern of the synthesized powders.
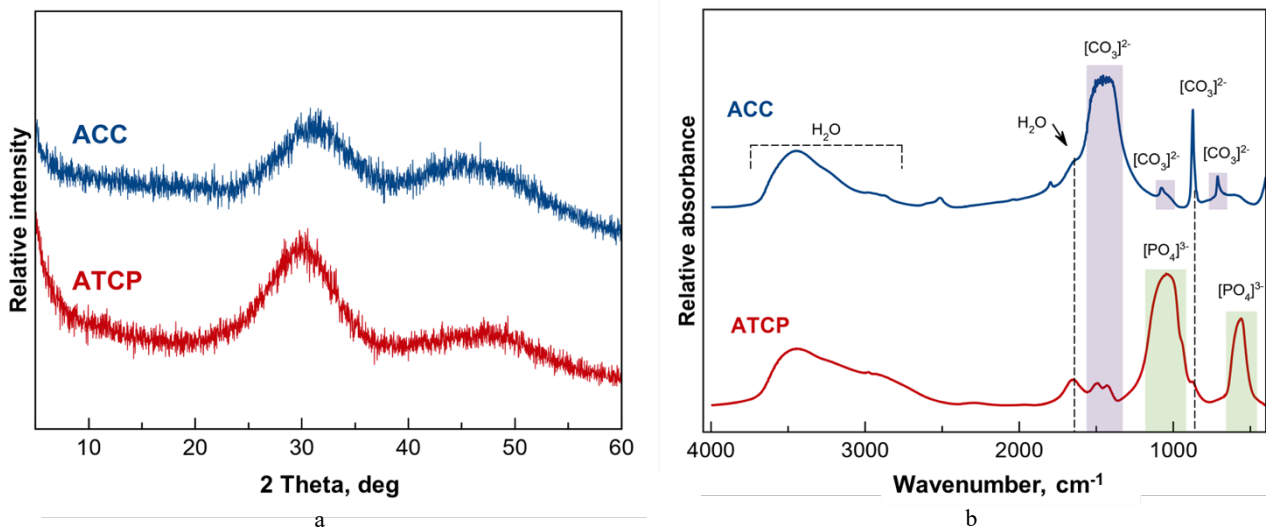
Fig. 1. a – XRD of amorphous calcium carbonate (ACC); b – amorphous tricalcium phosphate (ATCP) FTIR spectra showing characteristic spectral bands

Both phases show two low-intensity broad peaks at 30° and 45° 2theta indicating the amorphous nature of amorphous calcium carbonate (ACC) and amorphous tricalcium phosphate (ATCP). Further investigation by FTIR indicated an amorphous state and chemical characteristics of ACC and ATCP. FTIR spectral bands of the amorphous phase (see Fig. 1 b) are rounded (without any sharp peaks), characteristic of amorphous ACC and ATCP powders [27, 28]. Absorption bands of ACC are positioned at: 700 cm^{-1} ($v_4CO_3^{2-}$), 866 cm^{-1} ($v_2CO_3^{2-}$), 1050 cm^{-1} ($v_1CO_3^{2-}$), 1415 and 1505 cm^{-1} ($v_3CO_3^{2-}$) and 1670 and $3000-3500$ cm^{-1} (water bands) [27]. Absorption bands of ATCP are positioned at: 570 cm^{-1} (v_4 PO_4^{3-}), 866 cm^{-1} ($v_2CO_3^{2-}$), 1045 cm^{-1} ($v_3PO_4^{3-}$), 1415 and 1505 cm^{-1} ($v_3CO_3^{2-}$), 1670 and $3000-3500$ cm^{-1} (water bands) [28].

DTA showed the crystallization temperature of amorphous calcium carbonate and amorphous tricalcium phosphate. The first endothermic response was characteristic of the removal of water, Fig. 2 a. The exothermic events correspond to the crystallization of the amorphous phases: amorphous calcium carbonate crystallized first at $563-588$ K followed by the crystallization of amorphous tricalcium phosphate at $868-903$ K. Therefore, 588 K (315 °C) temperature was set for ACC and 903 K (630 °C) for ATCP. Powders were then characterized by XRD to ascertain that the crystallization was complete.

Fig. 2 b shows intense, sharp XRD peaks characteristic of the crystalline phase and the purity of precursors. Each diffraction peak was assigned to the characteristic reflections of calcite, α-tricalcium phosphate, and β-tricalcium phosphate (JCPDS card no. 04-008-0788, no. 04-010-4348 and no. 04-008-8714). No other significant phases appeared after the crystallization of ACC and ATCP.

3.2. Production of pellets and physicochemical characterization

Steam processing promoted a chemical reaction between calcium carbonate and tricalcium phosphate allotropes. Amorphous mixtures of calcium carbonate and tricalcium phosphate successfully induced apatite formation and showed a complete reaction to an apatite. A similar apatite product was achieved from the solid reactants added in crystalline form.

Fig. 3 a shows the XRD diffraction pattern of the steam processed pellets of amorphous and crystalline calcium carbonate and tricalcium phosphate powders. Each diffraction peak showed the characteristic reflections of hydroxyapatite (JCPDS card no. 01-074-0565).

The structural and chemical transformation to apatite was evaluated by Rietveld's analysis using the starting phases calcite (JCPDS card no. 04-008-0788) and β-tricalcium phosphate (JCPDS card no. 04-008-8714), and the best fit resulted from hydroxyapatite (JCPDS card no. 01-074-0565) and calcium-deficient hydroxyapatite phases (JCPDS card no. 00-046-0905).

A more detailed insight was provided from the results of Rietveld's analysis (Table 1) which indicated hydroxyapatite as the major phase and calcium-deficient hydroxyapatite as a secondary phase. With calcite and β-TCP at less than 1 mass%, these phases were considered as absent.

Table 1. Rietveld's analysis of steam processed pellets

Mass %	HA	CDHA	Calcite	β-TCP
MIX-1 (amorphous)	83.5 ± 2.2	15.7 ± 2.1	< 1	< 1
MIX-2 (crystalline)	75.7 ± 2.3	23.7 ± 2.3	< 1	< 1

The unit cell parameters of hydroxyapatite for MIX-1 were a = 0.9433 nm and c = 0.6884 nm, but for MIX-2: a = 0.9423 nm and c = 0.6889 nm. Results are in good agreement with the data found in the literature (HAp lattice parameters: a = 0.9430 nm, c = 0.6891 nm [29]. XRD data did not show carbonate substitution in the apatite structure. However, FTIR deconvolution revealed carbonate substitutions in phosphate and hydroxyl sites (Fig. 4). Apatite was successfully formed from amorphous and crystalline powders by steam processing. It should be noted that more hydroxyapatite formed from the amorphous starting powders than with the crystalline allotropes.
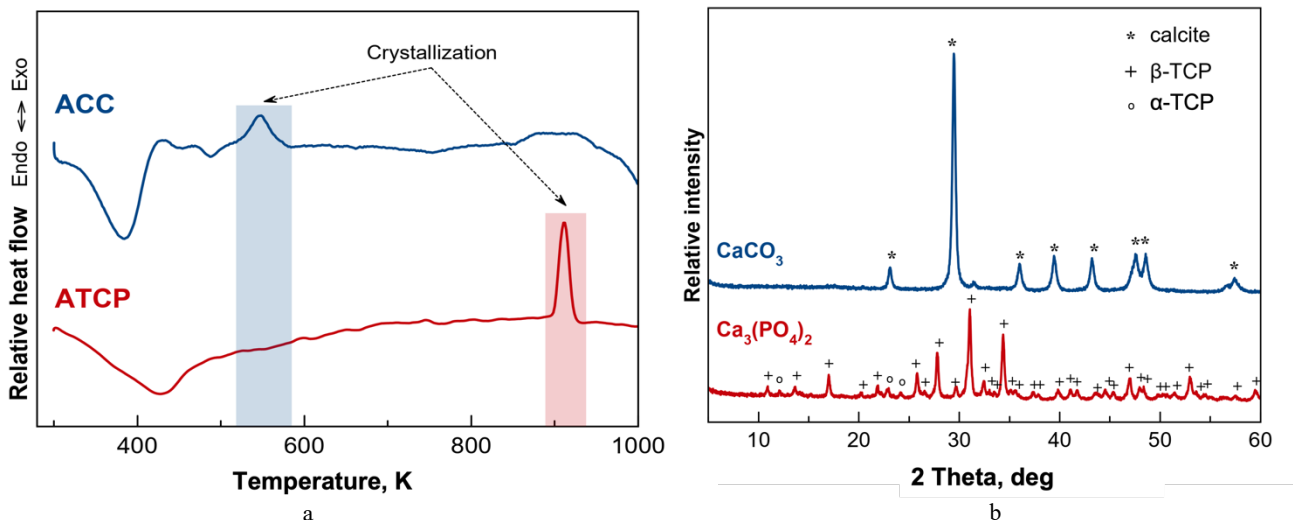
Fig. 2. Crystallization temperature of amorphous calcium carbonate (ACC) and amorphous tricalcium phosphate (ATCP): a – an exothermic event in DTA; b – XRD of the corresponding crystalline allotropes
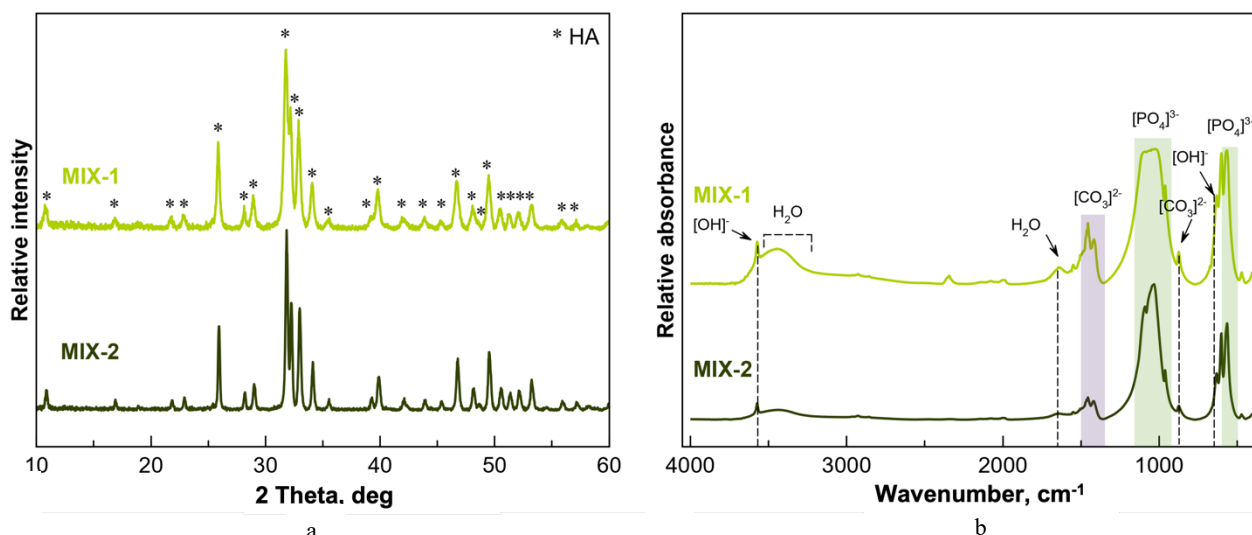
Fig. 3. Apatite reaction products from amorphous (MIX-1, light green) and crystalline powders (MIX-2, dark green): a – XRD; b – FTIR spectra

FTIR spectra and XRD data confirm the formation of apatite (Fig. 3 b) [30] that collates information on the structure and covalent bonding. FTIR absorption bands of MIX-1 and MIX-2 are positioned at: 570 cm^{-1} ($v_2PO_4^{3-}$), 866 cm^{-1} ($v_2CO_3^{2-}$), 1045 cm^{-1} ($v_3PO_4^{3-}$), 1415 and 1505 cm^{-1} ($v_3CO_3^{2-}$), 1670 and 3000 – 3500 cm^{-1} (water bands) and sharp OH$^-$ band at 3570 cm^{-1}.

Detailed analysis of the carbonate band at 800 – 900 cm^{-1} by deconvolution acquired information about possible carbonate ion substitutions: in the lattice (A-type substitution of OH$^-$ ion or B-type substitution in the phosphate site) and a third location not an apatitic substitution suggesting the existence of labile surface ions [30].

FTIR spectra deconvolution shows that amorphous precursors gave more carbonate in the phosphate site (B-type), however for the crystalline precursors more carbonate is shown to be in the nonapatitic region. It is not clear whether the higher hydroxyl content arises from the structural difference since the amorphous phase contained more adsorbed water, that was uniformly distributed in the pellet.

3.3. Change in pellet density and carbonate amount

Results showed a decrease in bulk density (Table 2), which could be assigned to the partial dissolution of pellets or sealing of pores during steam processing. This will be discussed in more detail in the next section.

Carbon mass fraction analysis followed the changes in carbonate amount after steam processing. For the initial insight, the crystalline powder blend (MIX-2) was chosen because of the instability of amorphous powders, especially, amorphous calcium carbonate. Therefore, it was not possible to heat the MIX-1 powder to 105 °C for 2 hours without crystallization of amorphous calcium carbonate in the process. However, it was possible to measure the carbonate amount after the steam processing of both MIX-1 and MIX-2 pellets. Table 2 shows that about 43 % of the carbonate was lost during the steam processing.
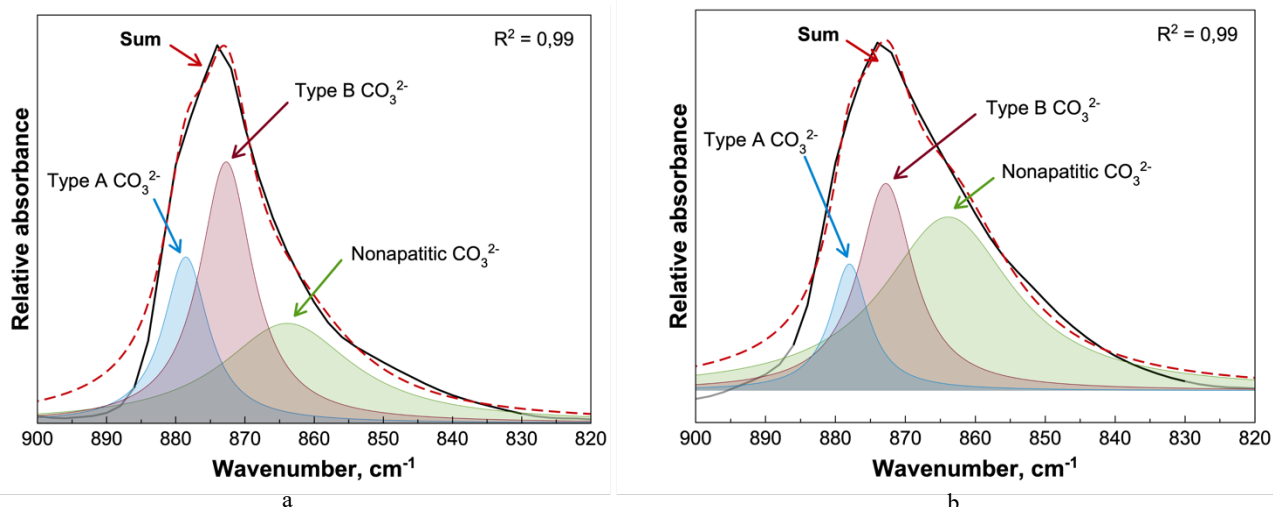
Fig. 4. FTIR spectra deconvolution of steam processed pellets consisting of: a – amorphous precursors (MIX-1); b – crystalline precursors (MIX-2) showing more carbonate in the apatite structure from the use of amorphous precursors

Table 2. Decrease in density and carbonate from steam processing

	Bulk density, g cm^{-3}		CO$_3$ amount, mass%	
	before SP	after SP	before SP	after SP
MIX-1	1.91 ± 0.02	1.87 ± 0.10	n/a	3.63 ± 0.02
MIX-2	1.94 ± 0.04	1.90 ± 0.06	5.98 ± 0.04	3.39 ± 0.01
SP – steam processing				

The intensity of the FTIR spectra carbonate band at 800–900 cm^{-1} is higher for the MIX-1 (amorphous precursors), which is in an agreement with the data provided by the carbon mass fraction analysis showing 3.63 mass% of carbonate after the steam processing, compared to a lower amount of 3.39 mass% of carbonate for MIX-2 (crystalline precursors).

4. DISCUSSION

This study showed that steam processing successfully synthesized crystalline apatite from mechanically blended nanosized calcium carbonate and tricalcium phosphate powders without waste products and at a very low reaction sintering temperature of 180 °C. Compared to the wet precipitation synthesis of calcium nitrate and ammonium phosphate solutions, no waste products evolved.

It was expected that carbonate ions would be incorporated into the apatite lattice through the steam processing of mechanically blended nanosized powders. Ideally, this would lead to a carbonate apatite resembling the inorganic component of the bone [31]. Nevertheless, the calculated carbonate amount in the product was 3.4 %, very close to the 3.3 % seen in minerals inside the human body [32], the steam processing proved successful in producing hydroxyapatite and calcium-deficient apatite instead of carbonate apatite, as shown by XRD. Hydroxyapatite lattice unit cell parameters are very similar to the data found in the literature [29], therefore no significant lattice deformations have occurred. However, FTIR deconvolution data revealed that amorphous precursors allowed the incorporation of carbonate into the phosphate site more than the crystalline precursors. Both precursors showed a large peak characteristic of nonapatitic labile surface carbonate (the peak area of MIX-1 was 0.92 and 0.97 for MIX-2). This could mean that the XRD was not able to detect such small amounts of A-type and B-type substituted carbonate apatite. Following FTIR spectra deconvolution, it can be suggested that carbonate ions might be adsorbed onto the surface of the apatitic core in the nonapatitic hydrated surface layer as labile carbonate ions possibly due to the influence of water molecules in steam processing ejecting the carbonate from the structure to the surface. The indication of calcium-deficient hydroxyapatite as the secondary phase indicated by XRD Rietveld's analysis might be associated with carbonate inclusion in the apatite structure.

Higher energy held by the amorphous phase, ideally, could be redirected to a chemical reaction of the mixed powders to crystallize into apatite at a lower temperature by steam processing. DTA allowed the determination of the crystallization temperature of amorphous calcium carbonate and amorphous tricalcium phosphate and the thermal reaction to form apatite. For amorphous tricalcium phosphate, the crystallization temperature is quite high (610 °C), so for the final transition into apatite, a higher temperature is expected. Steam processing allowed using a significantly lower temperature (180 °C) to produce a crystalline apatite.

Furnace heating was not capable of producing an apatite due to the thermal instability of calcium carbonate. At 700 °C (30 min; in a preheated furnace) apatite did not form (supplementary material XRD data 1 and 2). After heating at 1000 °C for 30 min in the tube furnace (supplementary material XRD data 3), the peaks in the XRD pattern did not match either of the apatite phases. The decomposition of calcium carbonate to calcium oxide prevented the formation of apatite. The comparison of amorphous and crystalline mechanically blended and compressed powders after steam processing showed purer hydroxyapatite for the amorphous precursors (approximately 7 mass% higher conversion to hydroxyapatite) than for the crystalline precursors. It should be noted that Rietveld's analysis provided a better fit for the amorphous blend (MIX-1) than for crystalline starting powders in MIX-2 (χMIX-1 = 1.08 and χMIX-2 = 1.20). Steam processing allowed a reduction of the temperature and obtained a crystalline apatite, utilizing the enclosed energy of the amorphous phase.

4.1. Mechanical integrity and porous constructs

Bulk density was measured to investigate further compaction of pressed pellets of mixed amorphous and crystalline nanosized powders. Results showed a decrease in density from steam processing. An explanation of this could be the changes in the content of water. Amorphous starting powders contained water as seen in FTIR spectra. It is possible, that water evaporated during steam processing thereby lowering the mass of the pellet, to a lower-density pellet. To further study the role of water in this process, chemically modified water could be used to infiltrate it in the powder at a known amount and then hydrothermally process the pressed pellets.

The solubility of calcium carbonate and tricalcium phosphate allotropes may also affect the density. The steam processing involves steam and therefore could initiate the dissolution of pore walls at elevated temperature and pressure inside the hydrothermal vessel. Dissolution could increase the density of pore walls. The higher solubility of calcium carbonate (pKa = 6.0 of the amorphous, pKa = 8.4 of the crystalline phase) [33] and tricalcium phosphate (pKa = 28.9 of the crystalline phase) [18] compared to hydroxyapatite (pKa = 58.4) [18] provides the basis for a denser pore wall. Higher pore wall densities could be further studied by nanoindentation by examining hardness or by looking at the pore cross-section area under a scanning electron microscope. It is not known whether the interaction of water with the porous solid could have dissolved some solid leading to a higher concentration of calcium and phosphate in the initial water.

Despite the lack of attention on porosity, the present nano to micro-scale porosity can be supplemented with larger connected pores. A soluble interconnected salt network integrated into the mechanically pressed powder blend could be easily dissolved to introduce larger-sized pores [34]. The steam processing would then preferentially dissolve the salt network to reveal the underlying pore walls

where the solubility of the powder blend may strengthen the remaining powder by a process of dissolution. This approach marks the next step in the possible use of steam processing for adding pore networks into the pellet.

Since 1952, steam was not used in hydrothermal synthesis, however, the conducted study diverged from initial practices of using a liquid phase (such as phosphoric acid [4], ammonium dibasic phosphate solution [7, 12], and nitrate solution [8]) instead of steam. This study has returned to the approach of the first discoveries together with cold sintering to provide a new result: steam processing successfully used the nanosized powder mixtures to obtain 99 % apatite, consisting of hydroxyapatite and calcium-deficient apatite.

Control of the quantity of each apatite phase could lead to a new type of apatite material and alter the proportion of hydroxyapatite and calcium-deficient apatite. It is worthwhile mentioning that it is rare to have two such apatites mutually co-existent. Usually, a solid solution is formed with a clearly defined apatite composition.

4.2. The future green potential of steam processing

The development of materials is controlled by the composition and the processing route. A change in the parameters will also change the chemical composition. For CO_3^{2-} incorporation into the PO_4^{3-} site, Ca^{2+} should theoretically be released from the apatite structure resulting in calcium-deficient apatite (Ca/P smaller than 1.67 [35]):

$$2CO_3^{2-} + \square = 2\ PO_4^{3-} + Ca^{2+}. \qquad (4)$$

However, a vacancy is needed for CO_3^{2-} incorporation into the OH^- site supporting the formation of hydroxyapatite [36]:

$$CO_3^{2-} + \square = 2OH^-. \qquad (5)$$

By changing, for example, the steam processing time, the amount of CO_3^{2-} retained inside the structure could change or otherwise be released to the surface of apatite.

Methods to improve carbonate ion retention are of interest to further reduce the CO_2 gas pollution, as the results show that half of the carbonate from calcium carbonate is lost during processing.

It would be interesting to see how a higher carbonate amount changes the possibility of forming appatite and the associated kinetics. This study used calcium carbonate and tricalcium phosphate only in a molar ratio of 1:3, respectively. Carbonate is a major substituent in natural apatites [37], however in synthetic apatites carbonate has been incorporated into apatite up to 20 mass% [38 – 42]. The solid solubility and impact on steam processing are yet unknown.

The cold-sintering process [20, 21] is related to steam processing and so an understanding of steam-processed powders could help interpret the apatites formed during cold sintering. This densification strategy is an easy and affordable method that utilizes additional uniaxial pressure, an elevated, but low temperature, and moistened powder. Previous research, involving amorphous calcium phosphate powders has reported difficulties maintaining the metastable phase during the sintering process [43 – 46]: for amorphous apatite coating 125 °C was enough to crystallize the amorphous material under the influence of water vapor, 150 °C was determined to be the temperature at which ACP crystallizes during spark plasma sintering and also the temperature at which ACP crystallizes during cold-sintering process. This leads to a discovery: can this very similar cold-sintering process be used to crystallize calcium carbonate and tricalcium phosphate powders blends into an apatite significantly increasing the density of the material?

In this study, only calcium carbonate and tricalcium phosphate powders were explored in terms of steam processing, however, various polymorphs such as calcite, vaterite, aragonite, the hydrated phases [26, 47] and natural sources of calcium carbonate (minerals deposits, eggshells, corals [48], and fish bones [49]) could be investigated further for this reaction. The kinetics of the reaction need to be determined for different forms of calcium carbonate as well as different calcium phosphate sources such as monetite ($CaHPO_4$). Herein lies an array of reactions to produce new materials by steam processing.

5. CONCLUSIONS

Steam processing of compacted powders proved to be successful in the production of 99% of the crystalline apatite phase for both amorphous and crystalline calcium carbonate and tricalcium phosphate starting powders. The resulting solid was a biphasic apatite consisting of 73-86% hydroxyapatite and 14 – 26 % of calcium-deficient hydroxyapatite.

Amorphous precursors allowed higher incorporation of carbonate in the phosphate site, however, the crystalline precursors showed relatively large nonapatitic carbonate presence, as determined by FTIR deconvolution.

Carbonate presence in the product after steam processing was higher for the MIX-1 (3.63 mass%), than MIX-2 (3.39 mass%), therefore approving data gained from FTIR spectra deconvolution.

A decrease in bulk density showed that steam processing cannot be used to increase the density of green body pellets, but the desired density should be achieved from the pre-compaction stage.

Steam processing as a second stage for apatite synthesis after acquiring precursors can be viewed as a greener method to synthesize apatite limiting significant chemical waste.

This method has great potential to utilize materials derived from renewable sources such as eggshell waste to produce apatite in an environmentally safer way.

REFERENCES

1. **Szcześ, A., Hołysz, L., Chibowski, E.** Synthesis of Hydroxyapatite for Biomedical Applications *Advances in Colloid and Interface Science* 249 2017: pp. 321 – 330. https://doi.org/10.1016/j.cis.2017.04.007

2. **Holland, H.D.** Hydrothermal Processes. In: Petrology. Boston, MA: Springer US, 1990: pp. 218 – 223. https://doi.org/10.1007/0-387-30845-8_97

3. **Wyart, J.** Hydrothermal Synthesis of Minerals *Discuss Faraday Society* 5 1949: pp. 323 – 324. https://doi.org/10.1039/DF9490500323

4. **Catherine, H., Skinner, W.** Studies in the Basic Mineralizing System, CaO-P2O5-H2O *Calcified Tissue Research* 14(1) 1974: pp. 3 – 14. https://doi.org/10.1007/BF02060279

5. **Gross, K.A., Komarovska, L., Viksna, A.** Efficient Zinc Incorporation in Hydroxyapatite through Crystallization of an Amorphous Phase Could Extend the Properties of Zinc Apatites *Journal of the Australian Ceramic Society* 49 (2) 2013: pp. 129 – 135. https://www.researchgate.net/publication/236890177

6. **Shi, D., Tong, H., Liv, M., Luo, D,. Wang, P., Xu, X., Han, Z.** Optimization of Hydrothermal Synthesis of Hydroxyapatite from Chicken Eggshell Waste for Effective Adsorption of Aqueous Pb(II) *Environmental Science and Pollution Research* 28 (41) 2021: pp. 58189 – 58205. https://doi.org/10.1007/s11356-021-14772-y

7. **Shi, Y., Pan, T., Zhu, W., Yan, C., Xia, Z.** Artificial Bone Scaffolds of Coral Imitation Prepared by Selective Laser Sintering *Journal of the Mechanical Behavior of Biomedical Materials* 104 2020: pp. 103664 – 103675. https://doi.org/10.1016/j.jmbbm.2020.103664

8. **Tampieri, A., Ruffini, A., Ballardini, A., Montesi, M., Panseri, S., Salamanna, F., Fini, M., Sprio, S.** Heterogeneous Chemistry in the 3-D State: An Original Approach to Generate Bioactive, Mechanically-Competent Bone Scaffolds *Biomaterials Science* 7 (1) 2019: pp. 307 – 321. https://doi.org/10.1039/C8BM01145A

9. **Yanan, T., Teng, G., Guiyun, R.** Preparation and Biological Properties of Zinc-Doped Hydroxyapatite *Chinese Journal of Tissue Engineering Research* 26 (16) 2022: pp. 2727 – 2733. https://doi.org/10.12307/2022.264

10. **Nuzulia, N.A., Siregar, F.A., Sari, Y.W.** Hydrothermal Synthesis of Fluoride-Substituted Calcium Phosphate in Supersaturation Condition *In: AIP Conference Proceedings* 2346 (020008) 2021: pp. 1 – 6. https://doi.org/10.1063/5.0048192

11. **Brill, R., Melczynski, I.** Hydrothermal Sintering *Angewandte Chemie International Edition in English* 3 (2) 1964: pp. 133 – 133. https://doi.org/10.1002/anie.196401331

12. **Hirano, S.I., Somiya, S.** Hydrothermal Reaction Sintering of Pure Cr2O3 *Journal of the American Ceramic Society* 59 (11 – 12) 1976: pp. 534 – 534. https://doi.org/10.1111/j.1151-2916.1976.tb09432.x

13. **Yamasaki, N., Yanagisawa, K., Nishioka, M., Kanahara, S.** A Hydrothermal Hot-Pressing Method: Apparatus and Application *Journal of Materials Science Letters* 5 (3) 1986: pp. 355 – 356. https://doi.org/10.1007/BF01748104

14. **Riman, R.E., Atakan, V.** Method of Hydrothermal Liquid Phase Sintering of Ceramic Materials and Products Derived Therefrom, U.S. Patent. 8,313,802, 2 2012: pp. 1 – 18.

15. **Agrawal, D.K.** Microwave Processing of Ceramics *Current Opinion in Solid State and Materials Science* 3 (5) 1998: pp. 480 – 485. https://doi.org/10.1016/S1359-0286(98)80011-9

16. **Yang, G., Park, S.J.** Conventional and Microwave Hydrothermal Synthesis and Application of Functional Materials: A Review *Materials (Basel)* 12 (7) 2019: pp. 1177 – 1195. https://doi.org/10.3390/ma12071177

17. **Pyldme, M., Utsal, K., Aruvali, J., Arnold, M., Paulik, F.** Investigation of Phase Transformations in Thermal Processing of Phosphate Rock *Journal of Thermal Analysis* 36(5). 1990: pp. 1699 – 1705. https://doi.org/10.1007/BF01913416

18. **Yanagisawa, K., Kim, J.H., Sakata, C., Onda, A., Sasabe, E., Yamamoto, T., Matamoros-Veloza, Z., Rendón-Angeles, J.C.** Hydrothermal Sintering under Mild Temperature Conditions: Preparation of Calcium-Deficient Hydroxyapatite Compacts *Zeitschrift fur Naturforschung – Section B Journal of Chemical Sciences* 65 (8) 2010: pp. 1038 – 1044. https://doi.org/10.1515/znb-2010-0810

19. **Chow, L.** Solubility of Calcium Phosphates *Monographs in Oral Science* 18 2001: pp. 94 – 111. https://doi.org/10.1159/000061650

20. **Guo, H., Baker, A., Guo, J., Randall, C.A.** Cold Sintering Process: A Novel Technique for Low-Temperature Ceramic Processing of Ferroelectrics *Journal of the American Ceramic Society* 99 (11) 2016: pp. 3489 – 3507. https://doi.org/10.1111/jace.14554

21. **Guo, J., Guo, H., Baker, A.L., Lanagan, M.T., Kupp, E.R., Messing, G.L., Randall, C.A.** Cold Sintering: A Paradigm Shift for Processing and Integration of Ceramics *Angewandte Chemie International Edition* 55 (38) 2016: pp. 11457 – 11461. https://doi.org/10.1002/anie.201605443

22. **Rey, C., Combes, C., Drouet, C., Grossin, D.** Bioactive Ceramics: Physical Chemistry *In: Comprehensive Biomaterials* 2011: pp. 187 – 221. https://doi.org/10.1016/B978-0-08-055294-1.00178-1

23. **Mann, S.** Biomineralization: principles and Concepts in Bioinorganic Materials Chemistry, Oxford University Press, NY, 2001: pp. 1 – 216.

24. **Pudule, A.A., Gross, K.A., Tonsuaadu, K., Kuzmenko, I., Ilavsky, J.** Crystallization of Amorphous Calcium Compounds underpins Further Growth of Crystallinity Controlled Biomaterials *In: The 78th International Scientific Conference of the University of Latvia Chemistry Section*, Riga: University of Latvia, 2020: p. 58.

25. **Healy, K., Hytmacher, D.W., Grainer, D.W., Kirkpatrick, C.J.** Comprehensive Biomaterials II. Elsevier, USA, 2017.

26. **Ihli, J., Wong, W.C., Noel, E.H., Kim, Y.Y., Kulak, A.N., Christenson, H.K., Duer, M.J., Meldrum, F.C.** Dehydration and Crystallization of Amorphous Calcium Carbonate in Solution and in Air *Nature Communications* 28 (5) 2014: pp. 3169 – 3179. https://doi.org/10.1038/ncomms4169

27. **Rodriguez-Blanco, J.D., Shaw, S., Benning, L. G.** The Kinetics and Mechanisms of Amorphous Calcium Carbonate (ACC) Crystallization to Calcite, via Vaterite *Nanoscale* 3 (1) 2011: pp. 265 – 271.

https://doi.org/10.1039/c0nr00589d

28. **Berzina-Cimdina, L., Borodajenko, N.** Research of Calcium Phosphates using Fourier Transform Infrared Spectroscopy *Infrared Spectroscopy – Materials Science, Engineering and Technology* 2012: pp. 123 – 148.
https://doi.org/10.5772/36942

29. **Dorozhkin, S.V., Epple, M.** Biological and Medical Significance of Calcium Phosphates *Angewandte Chemie International Edition* 41 (17) 2002: pp. 3130 – 3146.
https://doi.org/10.1002/1521-3773(20020902)41:17<3130::aid-anie3130>3.0.co;2-1

30. **Rey, C., Combes, C., Drouet, C., Lebugle, A., Sfihi, H., Barroug, A.** Nanocrystalline Apatites In Biological Systems: Characterisation, Structure and Properties *Materialwissenschaft und Werkstofftechnik* 38 (12) 2007: pp. 996 – 1002.
https://doi.org/10.1002/mawe.200700229

31. **Ishikawa, K., Hayashi, K.** Carbonate Apatite Artificial Bone *Science and Technology of Advanced Materials* 22 (1) 2021: pp. 683 – 694.
https://doi.org/10.1080/14686996.2021.1947120

32. **Zipkin, I.** The Inorganic Composition of Bones and Teeth. In H. Schraer (ed.): Biological Calcification: Cellular and Molecular Aspects, Springer, NY, 1970: pp. 63 – 103.
https://doi.org/10.1007/978-1-4684-8485-4_3

33. **Rodriguez-Navarro, C., Kudłacz, K., Cizer, Ö., Ruiz-Agudo, E.** Formation of Amorphous Calcium Carbonate and Its Transformation into Mesostructured Calcite *CrystEngComm* 17 (1) 2015: pp. 58 – 72.
https://doi.org/10.1039/C4CE01562B

34. **Gross, K.A., Rodríguez-Lorenzo, L.M.** Biodegradable Composite Scaffolds with an Interconnected Spherical Network for Bone Tissue Engineering *Biomaterials* 25 (20) 2004: pp. 4955 – 4962.
https://doi.org/10.1016/j.biomaterials.2004.01.046

35. **Wopenka, B., Pasteris, J.D.** A Mineralogical Perspective on the Apatite in Bone *Materials Science and Engineering: C* 25 (2) 2005: pp. 131 – 134.
https://doi.org/10.1016/j.Msec.2005.01.008

36. **Pan, Y., Fleet, M.E.** Compositions of the Apatite-Group Minerals: Substitution Mechanisms and Controlling Factors *In: Phosphates: Geochemical, Geobiological and Materials Importance De Gruyter Mouton* 2019: pp. 13 – 50.
https://doi.org/10.2138/rmg.2002.48.

37. **Smith, J.P., Lehr, J.R.** An X-Ray Investigation of Carbonate Apatites *Journal of Agricultural and Food Chemistry* 14 (4) 1996: pp. 342 – 349.
https://doi.org/10.1021/jf60146a004

38. **Landi, E., Tampieri, A., Celotti, G., Vichi, L., Sandri, M.** Influence of Synthesis and Sintering Parameters on the Characteristics of Carbonate Apatite *Biomaterials* 14 (4) 2004: pp. 1763 – 1770.
https://doi.org/10.1016/j.biomaterials.2003.08.026

39. **Barralet, J.E., Best, S.M., Bonfield, W.** Effect of Sintering Parameters on the Density and Microstructure of Carbonate Hydroxyapatite *Journal of Materials Science: Materials in Medicine* 11 (11) 2000: pp. 719 – 724.
https://doi.org/10.1023/A:1008975812793

40. **Bonfield, W., Gibson, I.R.** Novel Synthesis and Characterization of an AB-Type Carbonate-Substituted Hydroxyapatite *Journal of Biomedical Materials Research* 59 (4) 2002: pp. 697 – 708.
https://doi.org/10.1002/jbm.10044

41. **Ortali, C., Julien, I., Vandenhende, M., Drouet, C., Champion, E.** Consolidation of Bone-Like Apatite Bioceramics by Spark Plasma Sintering of Amorphous Carbonated Calcium Phosphate at Very Low Temperature *Journal of European Ceramic Society* 38 2018: pp. 2098 – 2109.
https://doi.org/10.1016/j.jeurceramsoc.2017.11.051

42. **Tadic, D., Peters, M., Epple, M.** Continuous Synthesis of Amorphous Carbonated Apatites *Biomaterials* 23 (12) 2002: pp. 2553 – 2559.
https://doi.org/10.1016/s0142-9612(01)00390-8

43. **Cao, Y.** Water Vapour-Treated Hydroxyapatite Coatings after Plasma Spraying and their Characteristics *Biomaterials* 17 (4) 1996: pp. 419 – 424.
https://doi.org/10.1016/0142-9612(96)89658-x

44. **Sato, M., Slamovich, E.B., Webster, T.J.** Enhanced Osteoblast Adhesion on Hydrothermally Treated Hydroxyapatite/Titania/Poly(Lactide-Co-Glycolide) Sol–Gel Titanium Coatings *Biomaterials* 26 (12) 2005: pp. 1349 – 1357.
https://doi.org/10.1016/j.biomaterials.2004.04.044

45. **Balasundaram, G., Sato, M., Webster, T.J.** Using Hydroxyapatite Nanoparticles and Decreased Crystallinity to Promote Osteoblast Adhesion Similar to Functionalizing with RGD *Biomaterials* 27 (12) 2006: pp. 2798 – 2805.
https://doi.org/10.1016/j.biomaterials.2005.12.008

46. **Rubenis, K., Zemjane, S., Vecstaudza, J., Bitenieks, J., Locs, J.** Densification of Amorphous Calcium Phosphate using Principles of Cold Sintering Process *Journal of the European Ceramic Society* 4 (1) 2020: pp. 912 – 919.
https://doi.org/10.1016/j.jeurceramsoc.2020.08.074

47. **Zou, Z., Habraken, W.M., Matveeva, G., Jensen, A.S., Bertinetti, L., Hood, M.A., Sun, C., Gilbert, P.U.P.A., Polishchuk, I., Pokroy, B., Mahamid, J., Politi, Y., Weiner, S., Werner, P., Bette, S., Dinnebier, R., Kolb, U., Zolotoyabko, E., Fratzl, P.** Solid-State Chemistry. A Hydrated Crystalline Calcium Carbonate Phase: Calcium Carbonate Hemihydrate *Science* 363 (6425) 2019: pp. 396 – 400.
https://doi.org/10.1126/science.aav0210

48. **White, R.A., Weber, J.N., White, E.W.** Replamineform: A New Process for Preparing Porous Ceramic, Metal, and Polymer Prosthetic Materials *Science* 176 (4037) 1972: pp. 922 – 924.
https://doi.org/10.1126/science.176.4037.922

49. **Xu, Y., Ye, J., Zhou, D., Su, L.** Research Progress on Applications of Calcium Derived from Marine Organisms *Scientific Reports* 10 (1) 2020: pp. 18425 – 18433.
https://doi.org/10.1038/s41598-020